

Received:
17 March 2016Revised:
12 August 2016Accepted:
17 October 2016

© 2016 The Authors. Published by the British Institute of Radiology under the terms of the Creative Commons Attribution-NonCommercial 4.0 Unported License <http://creativecommons.org/licenses/by-nc/4.0/>, which permits unrestricted non-commercial reuse, provided the original author and source are credited.

Cite this article as:

Wang X, Joseph AA, Kalentev O, Merboldt K-D, Voit D, Roeloffs VB, et al. High-resolution myocardial T_1 mapping using single-shot inversion recovery fast low-angle shot MRI with radial undersampling and iterative reconstruction. *Br J Radiol* 2016; **89**: 20160255.

FULL PAPER

High-resolution myocardial T_1 mapping using single-shot inversion recovery fast low-angle shot MRI with radial undersampling and iterative reconstruction

¹XIAOQING WANG, MSc, ^{1,2}ARUN A JOSEPH, PhD, ¹OLEKSANDR KALENTEV, PhD, ¹KLAUS-DIETMAR MERBOLDT, PhD, ¹DIRK VOIT, PhD, ¹VOLKERT B ROELOFFS, PhD, ¹MAAIKE VAN ZALK, PhD and ^{1,2}JENS FRAHM, PhD

¹Biomedizinische NMR Forschungs GmbH, Max-Planck Institut für Biophysikalische Chemie, Göttingen, Germany

²DZHK (German Centre for Cardiovascular Research), partner site Göttingen, Germany

Address correspondence to: Mr Xiaoqing Wang

E-mail: xwang1@gwdg.de

Objective: To develop a novel method for rapid myocardial T_1 mapping at high spatial resolution.

Methods: The proposed strategy represents a single-shot inversion recovery experiment triggered to early diastole during a brief breath-hold. The measurement combines an adiabatic inversion pulse with a real-time readout by highly undersampled radial FLASH, iterative image reconstruction and T_1 fitting with automatic deletion of systolic frames. The method was implemented on a 3-T MRI system using a graphics processing unit-equipped bypass computer for online application. Validations employed a T_1 reference phantom including analyses at simulated heart rates from 40 to 100 beats per minute. *In vivo* applications involved myocardial T_1 mapping in short-axis views of healthy young volunteers.

Results: At 1-mm in-plane resolution and 6-mm section thickness, the inversion recovery measurement could be shortened to 3s without compromising T_1 quantitation. Phantom studies demonstrated T_1 accuracy and high precision for values ranging from 300 to 1500 ms and up to a heart rate of 100 beats per minute. Similar results were obtained *in vivo* yielding septal T_1 values of 1246 ± 24 ms (base), 1256 ± 33 ms (mid-ventricular) and 1288 ± 30 ms (apex), respectively (mean \pm standard deviation, $n = 6$).

Conclusion: Diastolic myocardial T_1 mapping with use of single-shot inversion recovery FLASH offers high spatial resolution, T_1 accuracy and precision, and practical robustness and speed.

Advances in knowledge: The proposed method will be beneficial for clinical applications relying on native and post-contrast T_1 quantitation.

INTRODUCTION

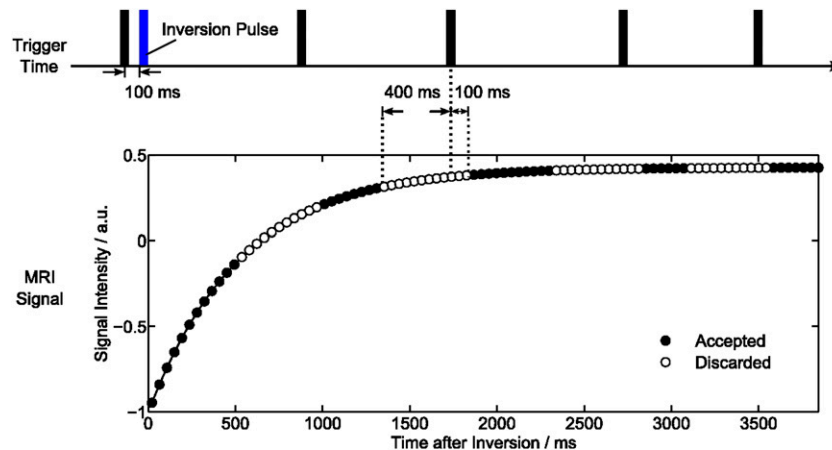
Tissue characterization by native myocardial T_1 mapping as well as quantitation of perfusion and extracellular volume after contrast administration are essential ingredients of Cardiovascular magnetic resonance imaging (CMR) investigations and commonly performed by inversion recovery (IR) methods using Fast low-angle shot (FLASH),^{1,2} Echo planar imaging (EPI)³ or Steady-state free precession (SSFP) readouts⁴ according to the Look-Locker technique.⁵ To date, respective applications commonly rely on a modified Look-Locker inversion (MOLLI) experiment⁶ or manifold derivatives therefrom (for a recent review of possibilities and limitations, see Kellman and Hansen⁷). In fact, despite widespread usage, most approaches still suffer from practical restrictions such as limited spatial resolution and/or compromised T_1 accuracy, so that further technical improvements are warranted.

Following the recommendations of the T_1 mapping Consensus Statement of the Society for Cardiovascular

Magnetic Resonance and CMR Working Group of the European Society of Cardiology,⁸ the basic requirements and clinical needs for cardiac T_1 mapping comprise (i) speed, *i.e.* single-shot applications with measuring times of a few seconds only, (ii) T_1 accuracy, *i.e.* validated T_1 values with small standard deviations and without dependency on heart rate, (iii) sufficiently high spatial resolution, *i.e.* about 1-mm in-plane resolution and (iv) practical robustness, *i.e.* no motion sensitivity and no image artefacts due to susceptibility problems, SSFP bandings or radial streakings.

This work describes a novel method which effectively meets all aforementioned challenges. It is based on a single-slice acquisition during a brief breath-hold (typically 3 s only) which combines a single-shot IR-FLASH technique with pronounced radial undersampling of individual frames, iterative reconstruction by non-linear inversion (NLINV)⁹ and conjugate gradient methods as previously

Figure 1. Myocardial T_1 mapping using single-shot inversion recovery FLASH with radial undersampling. Finger pulse trigger = black bar.



described^{10,11} and fitting of a diastolic T_1 map after deletion of systolic (*i.e.*, motion-affected) frames. The entire procedure is fully automatic and only requires triggering of the initial inversion pulse to early diastole. The results comprise both an image series representing the entire IR experiment and a colour-coded T_1 map where pixel intensities directly refer to T_1 values in milliseconds. The proposed T_1 mapping method complements previous real-time MRI acquisitions of cardiac function and flow^{12–15} which together bear the potential to develop a comprehensive real-time CMR examination.

METHODS AND MATERIALS

All measurements were performed on a human MRI system operating at 3 T (Magnetom® Prisma fit; Siemens Healthcare, Erlangen, Germany). Phantom measurements employed the 64-channel head coil, whereas human heart studies were performed using the 18-element thorax coil in combination with 12 elements of the 32-element spine coil. Six young subjects (two female, four male, age range 24–27 years) with no known illness [heart rate about 50–55 beats per minute (bpm)] were recruited among the students of the local university. Written informed

consent, according to the recommendations of the local ethics committee, was obtained from all subjects prior to MRI.

According to the T_1 mapping Consensus Statement,⁸ experimental validations of the proposed technique were performed at different simulated heart rates with the use of a commercial reference phantom (Diagnostic Sonar Ltd, Scotland, UK) consisting of six compartments with defined T_1 values surrounded by water. As suggested, a long-repetition time (TR) IR fast spin echo (FSE) sequence with 13 logarithmically spaced inversion times between 50 and 2300 ms served for T_1 determination [TR = 7.2 s, echo time (TE) = 12 ms, 6 echoes and measuring time = 50 min].

The procedures for cardiac T_1 mapping described below (*i.e.* data acquisition, image reconstruction and T_1 fitting) were implemented as an easy-to-use protocol on the MRI system by taking advantage of a bypass computer (sysGen/TYAN Octuple-GPU; Sysgen, Bremen, Germany) previously developed for real-time MRI^{9,15} and equipped with eight graphics processing units (NVIDIA® GeForce® GTX TITAN Black; NVIDIA, Santa Clara, CA). This bypass computer could be fully integrated into

Table 1. T_1 relaxation times for a reference phantom and simulated heart rates

T_1 , ms ^a	T_2 , ms ^b	Heart rate ^c				
		0	40	60	80	100
331 ± 11	101 ± 2	315 ± 13	315 ± 13	314 ± 13	316 ± 13	317 ± 16
494 ± 22	46 ± 2	476 ± 18	475 ± 18	475 ± 18	476 ± 20	479 ± 23
676 ± 19	81 ± 3	660 ± 25	659 ± 26	661 ± 27	663 ± 29	665 ± 31
857 ± 25	132 ± 5	850 ± 28	850 ± 28	852 ± 30	853 ± 30	853 ± 35
1225 ± 20	138 ± 4	1227 ± 34	1226 ± 34	1230 ± 36	1230 ± 37	1236 ± 38
1501 ± 23	166 ± 5	1511 ± 42	1513 ± 43	1513 ± 44	1516 ± 46	1517 ± 50

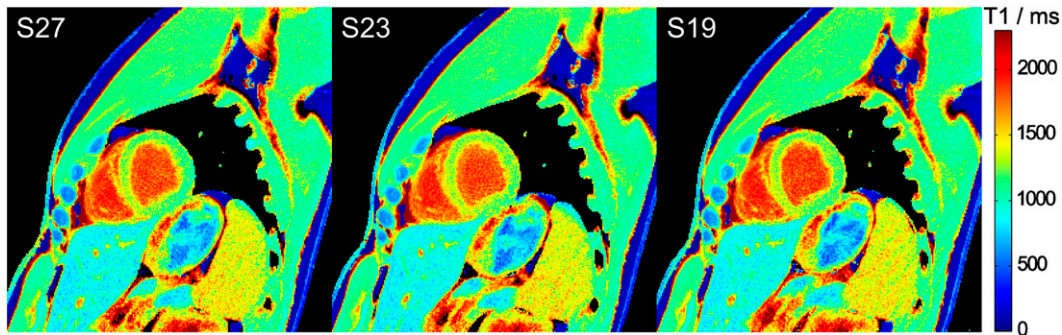
Single-shot inversion recovery FLASH was performed at 43-ms resolution (19 spokes) for a duration of 3 s.

^a T_1 values for a long-repetition time inversion recovery fast spin echo sequence.

^b T_2 values according to Sumpf et al.²⁹

^cSimulated heart rates (in beats per minute) correspond to the deletion of a 500-ms period (“systole”) in each cardiac cycle. No images are deleted for zero heart rate.

Figure 2. Myocardial T_1 maps for different temporal resolutions. Single-shot inversion recovery FLASH was performed with 27, 23 and 19 spokes per frame (*i.e.* acquisition times of 63, 52 and 43 ms) for a duration of 8 s.



the reconstruction pipeline of the commercial MRI system (Magnetom Prisma fit) by a single network connection. If the system software is compatible, the implementation takes less than an hour including installation of ready-to-use measuring protocols for cardiac T_1 mapping and other real-time CMR applications.

MRI acquisition and reconstruction

The chosen acquisition scheme for cardiac T_1 mapping is illustrated in Figure 1. In order to achieve maximum robustness and T_1 accuracy, a previously developed IR FLASH sequence¹⁰ was applied as a single-slice technique using a non-selective adiabatic 180° inversion pulse triggered to early diastole. The present study employed a simple and robust finger pulse trigger and a 100-ms delay to inversion. Although the method yields similar accuracy for a slice-selective inversion pulse when applied to stationary tissue (data not shown), cardiac T_1 mapping exclusively used a non-selective inversion pulse to minimize the effects of through-plane motion and myocardial perfusion.

Continuous image readout after inversion was based on a radial FLASH sequence with pronounced undersampling. Time-efficient spoiling of residual transverse magnetizations was accomplished by random radiofrequency (RF) phases.¹⁶ Cardiac T_1 maps were then acquired at a nominal in-plane resolution of $1.0 \times 1.0 \text{ mm}^2$ and 6-mm section thickness using a field of view = $256 \times 256 \text{ mm}^2$ in combination with a resolution of 512 complex data points per radial spoke (using two-fold oversampling). All spokes were homogeneously distributed over 360° , whereas five successive frames used complementary sets of spokes in sequential order. Other parameters were TR = 2.26 ms, TE = 1.47 ms and flip angle of 4° .

The number of spokes per frame varied from 27 to 23 and finally 19 spokes yielding a temporal resolution of 61, 52 and 43 ms, respectively. The total acquisition time was initially chosen to be 8 s but later reduced to 4 and 3 s.

Image reconstruction has previously been described for the case of non-cardiac T_1 mapping^{10,11} and employs the same iteratively regularized NLINV algorithm as developed for real-time MRI; for details, see Uecker et al.⁹ Apart from an advanced gradient-delay correction¹⁴ and data compression to 10 virtual channels based on a principal component analysis, the method takes advantage of some degree of spatial smoothness of coil sensitivities as well as of temporal regularization to the preceding frame. However, this latter term of the underlying cost function is downsized relative to the data consistency term by a factor of two during each iteration. The reconstruction ensures high temporal fidelity as demonstrated for a motion phantom rotating at defined speed¹⁷ and therefore does not compromise the resolution of contrast changes during inversion recovery.

The actual reconstruction process starts immediately after the end of data acquisition, first by a reverse NLINV reconstruction of the last 10 frames to obtain high-quality coil sensitivity maps using 6 iterations. Subsequently, the entire image series was reconstructed in the reverse order by fixing the coil sensitivities to those obtained by NLINV. The resulting linear inverse problem was solved by the iteratively regularized conjugate gradient method, again using six iterations.

Prior to T_1 fitting, the images were spatially filtered by a recently developed modified non-local means algorithm.¹⁸ The filter

Figure 3. Myocardial T_1 maps for different measurement durations. Single-shot inversion recovery FLASH was performed at 43 ms temporal resolution (19 spokes) for durations of 8, 4 and 3 s.

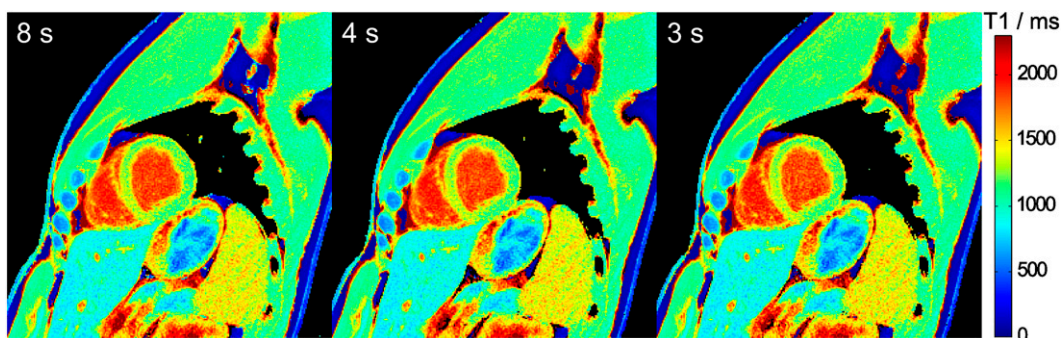


Table 2. Myocardial T_1 relaxation times for different temporal resolutions and measuring times

Spokes per frame	27	23	19
Temporal resolution ^a	61 ms	52 ms	43 ms
IR-FLASH measurement ^b	T_1 , ms ^c		
8 s	1253 ± 29	1254 ± 29	1253 ± 31
4 s	1252 ± 30	1254 ± 30	1253 ± 31
3 s	1254 ± 32	1257 ± 33	1256 ± 33

IR, inversion recovery.

^aNumber of spokes and acquisition time per frame.

^bTotal measuring time.

^cAveraged across subjects (mean ± standard deviation, $n = 6$).

preserves small isolated details and efficiently removes background noise [corresponding to a 60% signal-to-noise (SNR) improvement] without introducing blur, smearing or patch artefacts. This is accomplished by extending the conventional non-local means algorithm to adapt the influence of the original pixel value according to a simple measure for patch regularity. Detail preservation is improved by a compactly supported weighting kernel which closely approximates the commonly used exponential weight.

Temporal median filtering was only used for the purpose of displaying image series, whereas no temporal filter was used for T_1 mapping. The median filter extended over five frames to match the number of frames with different sets of spokes, e.g. in the studies of Uecker et al⁹ and Frahm et al.¹⁷ As illustrated in Figure 1, the influence of systolic motion on the fitting of a diastolic T_1 map was minimized by automatically deleting images

over a period of 500 ms starting from 400 ms prior to each finger pulse trigger signal.

T_1 quantitation

After reconstruction, spatial filtering and systolic deletion, the remaining complex images were fitted to the complex signal model²

$$M(t) = M_{\text{ini}} \left[\gamma - (1 + \gamma) \exp\left(\frac{-t}{T_1^*}\right) \right] \quad (1)$$

where M_{ini} is the initial complex signal after inversion; t is the central time point (*i.e.* radial spoke) of each frame during inversion recovery; γ is the ratio between the steady-state signal M_{ss} and M_{ini} ; and T_1^* is the shortened apparent T_1 due to multiple low flip-angle RF excitations. The same phase is assumed for M_{ss} and M_{ini} , which leads to four unknown real-valued parameters: $\text{Re}\{M_{\text{ini}}\}$, $\text{Im}\{M_{\text{ini}}\}$, γ and T_1^* . A pixelwise estimation was performed using the Trust-Region algorithm (Chapters 4.1 and 4.3 in the study of Nocedal and Wright¹⁹) based on the Dlib C++ library.²⁰ The algorithm performs an unconstrained minimization of the cost function defined by

$$\frac{1}{2} \sum_t ((\text{Re}\{M(t) - Y(t)\})^2 + (\text{Im}\{M(t) - Y(t)\})^2) \quad (2)$$

where Y corresponds to the vector of pixel intensities during inversion recovery. The iterative optimization was stopped if the relative difference of the objective function values between successive iterations was $< 10^{-5}$. T_1 was then calculated according to:²¹

$$T_1 = \frac{T_1^*}{\gamma} + 2\delta t \quad (3)$$

Figure 4. Cardiac images and T_1 maps (top) without and (bottom) with spatial filtering. Single-shot inversion recovery FLASH was performed at 43 ms temporal resolution (19 spokes) for a duration of 3 s. The images (magnified views) refer to an early time point after inversion, nulling of myocardial tissue and nulling of blood signal, respectively.

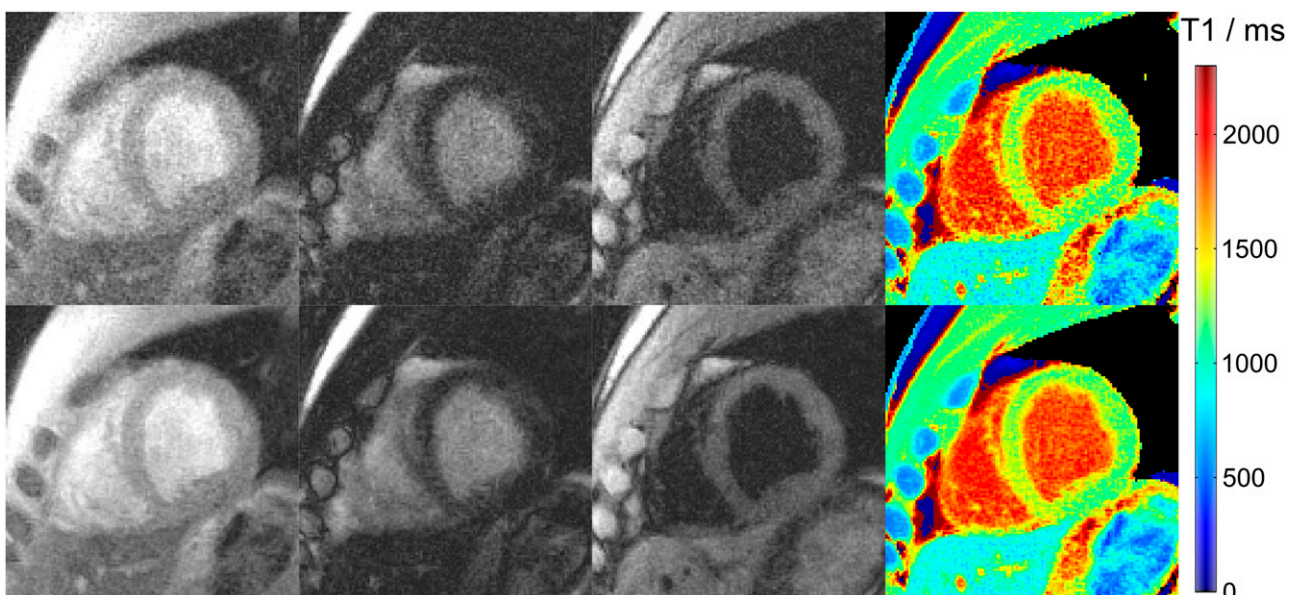
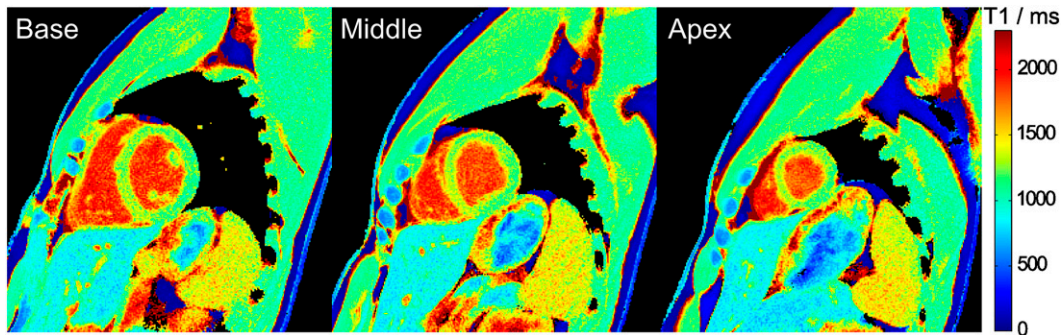


Figure 5. Myocardial T_1 maps of a basal, mid-ventricular and apical section. Single-shot inversion recovery FLASH was performed at 43 ms resolution (19 spokes) for a duration of 3 s.



with δt the delay between inversion and the start of data acquisition. In the present implementation, this period covered half of the inversion pulse (5 ms) and a following spoiler gradient (10 ms). For the assessment of myocardial T_1 values, the regions of interest were carefully selected to exclude contributions from the blood pool. These analyses were accomplished using the arrayShow tool²² in MATLAB® (MathWorks®, Natick, MA).

RESULTS

Table 1 summarizes T_1 relaxation times for a reference phantom. The data were acquired with the radial IR-FLASH method proposed for cardiac T_1 mapping (43-ms resolution and 3-s duration) at different simulated heart rates ranging from 40 to 100 bpm. Zero heart rate refers to T_1 fitting without deletion of any frames. A comparison with T_1 relaxation times obtained by a long-TR IR-FSE technique reveals excellent agreement for most (long) values, whereas two tubes with shorter values are slightly underestimated (maximum deviation 5%).

Figures 2 and 3 demonstrate cardiac T_1 maps for different numbers of spokes per frame, *i.e.* different temporal resolution, and different durations of the IR-FLASH measurement, respectively. In all cases, visual inspection reveals no detectable difference. This qualitative finding is confirmed by the quantitative analysis in Table 2.

The effect of filtering prior to T_1 fitting is demonstrated in Figure 4 comparing raw images and T_1 maps with and without application of a spatial filter. Figure 5 shows three T_1 maps for a single subject in a basal, mid-ventricular and apical short-axis section, whereas Figure 6 summarizes the mid-ventricular T_1 maps of all six subjects. A full cardiac image series which corresponds to the T_1 map in the mid-ventricular section of Figure 5 is available as Supplementary Video A. The quantitative results for all six subjects are summarized in Table 3 (septal T_1 values in a basal, mid-ventricular and apical section) and Table 4 (segmental T_1 values in a mid-ventricular section), respectively.

DISCUSSION

This work describes a novel method for myocardial T_1 mapping which offers accuracy, high spatial resolution, practical robustness and speed. The results indicate that myocardial T_1 mapping by IR-FLASH may be performed at a nominal resolution of

1.0 mm, a temporal resolution of 43 ms per frame and within a measuring time of only 3 s.

T_1 accuracy was confirmed in a phantom study providing reference T_1 values for a long-TR IR-FSE sequence. A slight

Figure 6. Myocardial T_1 maps of all six subjects (mid-ventricular section, magnified view). Single-shot inversion recovery FLASH was performed at 43 ms resolution (19 spokes) for a duration of 3 s.

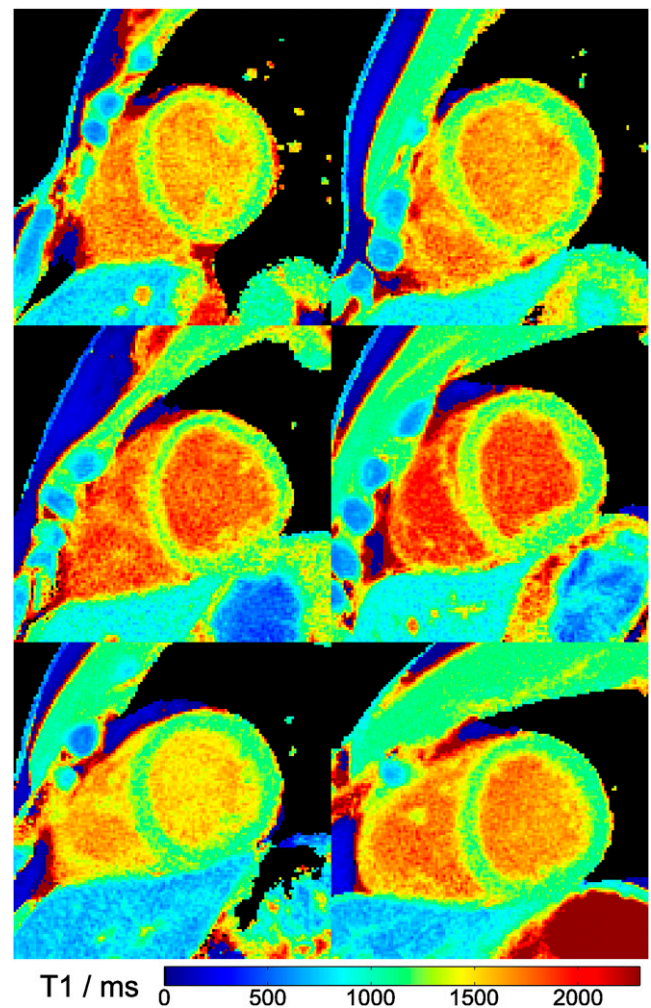


Table 3. T_1 relaxation times of the septal wall

Subject	Basal T_1 , #frames ^a	Mid-ventricular T_1 , #frames	Apical T_1 , #frames
#1	1250 ± 69/48	1256 ± 64/48	1298 ± 72/38
#2	1237 ± 60/48	1263 ± 54/47	1291 ± 58/47
#3	1270 ± 74/35	1287 ± 69/35	1332 ± 60/38
#4	1277 ± 71/47	1295 ± 61/49	1298 ± 50/47
#5	1215 ± 68/49	1209 ± 51/47	1256 ± 48/47
#6	1227 ± 61/49	1227 ± 51/47	1253 ± 46/48
Mean ^b	1246 ± 24	1256 ± 33	1288 ± 30
Kawel et al ²³		1286	
von Knobelsdorff-Brenkenhoff et al ²⁴	1157	1159	1181
Lee et al ²⁵		1315	

^a T_1 (in milliseconds, mean ± standard deviation in a region of interest covering most of the septal wall) for single-shot inversion recovery-FLASH at 43 ms resolution (19 spokes) and 3 s duration. #Frames refers to the number of images retained after deletion of systolic frames.

^bMean ± standard deviation across subjects.

underestimation of T_1 relaxation times for two tubes with values of about 500 and 675 ms coincides with the occurrence of the shortest T_2 relaxation times of 46 and 81 ms, respectively (compare Table 1). The slight deviation of T_1 values may therefore be due to a partial failure of the “reference” IR-FSE acquisition which extends to a maximum TE of 72 ms and thus may affect the image of compounds and tissues with short T_2 relaxation times. Similar effects are to be expected for IR methods with a SSFP readout module, because such sequences require relatively long T_2 relaxation times to build up sufficiently strong transverse coherences.

Apart from T_1 accuracy, the results in Table 1 confirm the independence of T_1 quantitation on the heart rate up to 100 bpm which effectively refers to the independence of T_1 on the number of fitted images after elimination of “systolic” frames. This advantageous behaviour reflects the fact that the highly undersampled radial FLASH readout ensures a sufficiently large number of frames for a proper sampling of the IR signal time course. T_1 precision was also demonstrated to be high both

in vitro and *in vivo*. It is characterized by small standard deviation values of 3–5% of the mean for phantom measurements and 4–8% for septal T_1 values (compare Tables 1–4). Moreover, the achieved T_1 mapping quality not necessarily depends on the use of filtering as shown by the comparison in Figure 4. Nevertheless, although high-quality T_1 maps may be obtained by fitting unfiltered images, the use of a new modified non-local means filter¹⁸ further improves the SNR of T_1 maps without the expense of blurring.

Although myocardial T_1 relaxation times found here were in general agreement with literature values, comparisons to previous results are compromised by numerous technical differences or even inadequacies. As an example, the present values are in the range of those reported in the study by Kawel et al²³ but slightly higher than in that by von Knobelsdorff-Brenkenhoff et al²⁴ and lower than in the study by Lee et al,²⁵ who all used similar MOLLI sequences. Of course, all techniques including the one proposed here suffer from some general limitations of the Lock-Locker approach which often are due to

Table 4. Regional myocardial T_1 relaxation times

Subject	Anterior T_1 , ms	Septal T_1 , ms	Inferior T_1 , ms	Lateral T_1 , ms
#1	1295 ± 70	1261 ± 70	1223 ± 95	1218 ± 70
#2	1191 ± 60	1259 ± 56	1245 ± 91	1157 ± 64
#3	1212 ± 62	1291 ± 68	1270 ± 89	1238 ± 69
#4	1224 ± 64	1304 ± 64	1230 ± 92	1217 ± 68
#5	1169 ± 56	1206 ± 59	1155 ± 79	1166 ± 57
#6	1173 ± 56	1234 ± 58	1171 ± 66	1156 ± 69
Mean ^a	1211 ± 47	1259 ± 36	1216 ± 44	1192 ± 36

T_1 (in milliseconds, mean ± standard deviation per standardized region of interest in a mid-ventricular section) for single-shot inversion recovery-FLASH at 43-ms resolution (19 spokes) and 3-s duration.

^aMean ± standard deviation across subjects.

the presence of residual motion both in plane and through plane. For example, diastolic circulation of blood within the ventricles leads to image intensities which violate the expected IR signal model and preclude a reliable fitting of blood T_1 relaxation times. Even myocardial movements may play a role during early diastolic phases. However, this mainly becomes a problem for motion-sensitive readouts such as SSFP sequences, whereas short-TE FLASH sequences as used here and recently proposed by others^{26,27} are much less affected. This is because SSFP sequences inherently rely on the establishment of phase coherence over multiple repetition intervals which is commonly precluded (*i.e.* spoiled) in the presence of motion, whereas FLASH sequences interrogate a pool of longitudinal magnetization with independent low-flip angle excitations that give rise to spin-density weighted images for the low flip angles used for T_1 mapping. In fact, when exploiting the additional motion robustness of radial encodings in the present implementation, preliminary trials of myocardial T_1 mapping during free breathing showed little if any qualitative and quantitative difference to breath-hold scans (data not shown). Thus, the proposed method seems to be robust enough to even work in patients who are unable to perform any breathing protocol.

Another factor contributing to myocardial T_1 values is the different access to high spatial resolution and the concomitant consideration of partial volume effects. Such problems have been reported for thin myocardial walls⁷ including the assessment of fibrosis in the peri-infarct zone as well as for the right ventricle.²⁸ These T_1 mapping studies using MOLLI techniques were performed at $1.4 \times 1.9 \times 8.0 \text{ mm}^3$ for low heart rates and $1.9 \times 2.3 \times 8.0 \text{ mm}^3$ at high heart rates.⁷ A higher resolution of $1.2 \times 1.2 \times 4 \text{ mm}^2$ was only achieved with the use of a segmented readout module after inversion which therefore required repetitive acquisitions and very long measuring times of 2.5 min

per T_1 map.²⁸ Another recent work using IR-FLASH employed a sliding-window reconstruction²⁷ at $1.17 \times 1.17 \times 8 \text{ mm}^3$ resolution, which was achieved by twofold zero-padding, *i.e.* an interpolation of the acquired resolution. To the best of our knowledge, the method proposed here is the first technique for myocardial T_1 mapping which offers $1.0 \times 1.0 \times 6.0 \text{ mm}^3$ resolution within a measuring time of only 3 s.

The most important limitation of this study is the small sample size. This is because the work represents a new technical development which requires basic validation with use of a T_1 reference phantom and a group of normal subjects. Obviously, this precedes any evaluation of the clinical utility of the proposed T_1 mapping in a large cohort of patients. Moreover, at this stage, widespread clinical applications are hampered by the fact that the technical solution requires dedicated software and hardware which so far is only available for MRI systems of the same manufacturer as used here. A remaining temporary restriction is the computational time needed for image reconstruction and T_1 fitting which currently takes about 13 s per T_1 map. Nevertheless, this may not necessarily block the clinical workflow, because a delayed reconstruction does not interfere with continuous acquisitions.

CONCLUSION

Myocardial T_1 mapping based on single-shot IR-FLASH with radial undersampling and iterative reconstruction as well as T_1 fitting with automated deletion of systolic frames meets most current clinical challenges. The proposed method warrants extensive clinical trials as it promises significant advantages for CMR studies which rely on native or post-contrast T_1 quantitation.

FUNDING

AAJ is supported by the DZHK (German Centre for Cardiovascular Research) and by the BMBF (German Ministry of Education and Research).

REFERENCES

- Haase A. Snapshot FLASH MRI. Applications to T1, T2, and chemical-shift imaging. *Magn Reson Med* 1990; **13**: 77–89. doi: <https://doi.org/10.1002/mrm.1910130109>
- Deichmann R, Haase A. Quantification of T1 values by SNAPSHOT-FLASH NMR imaging. *J Magn Reson* 1992; **96**: 608–12.
- Ordidge RJ, Gibbs P, Chapman B, Stehling MK, Mansfield P. High-speed multislice T1 mapping using inversion-recovery echo-planar imaging. *Magn Reson Med* 1990; **16**: 238–45. doi: <https://doi.org/10.1002/mrm.1910160205>
- Scheffler K, Hennig J. T1 quantification with inversion recovery TrueFISP. *Magn Reson Med* 2001; **45**: 720–3. doi: <https://doi.org/10.1002/mrm.1097>
- Look DC, Locker DR. Time saving in measurement of NMR and EPR relaxation times. *Rev Sci Instrum* 1970; **41**: 250–1. doi: <https://doi.org/10.1063/1.1684482>
- Messroghli DR, Radjenovic A, Kozerke S, Higgins DM, Sivanathan MU, Ridgway JP. Modified look-locker inversion recovery (MOLLI) for high-resolution T1 mapping of the heart. *Magn Reson Med* 2004; **52**: 141–6. doi: <https://doi.org/10.1002/mrm.20110>
- Kellman P, Hansen MS. T1-mapping in the heart: accuracy and precision. *J Cardiovasc Magn Reson* 2014; **16**: 2. doi: <https://doi.org/10.1186/1532-429X-16-2>
- Moon JC, Messroghli DR, Kellman P, Piechnik SK, Robson MD, Ugander M, et al. Myocardial T1 mapping and extracellular volume quantification: a Society for Cardiovascular Magnetic Resonance (SCMR) and CMR Working Group of the European Society of Cardiology consensus statement. *J Cardiovasc Magn Reson* 2013; **15**: 92. doi: <https://doi.org/10.1186/1532-429X-15-92>
- Uecker M, Zhang S, Voit D, Karaus A, Merboldt KD, Frahm J. Real-time MRI at a resolution of 20 ms. *NMR Biomed* 2010; **23**: 986–94. doi: <https://doi.org/10.1002/nbm.1585>
- Wang X, Roeloffs V, Merboldt KD, Voit D, Schätz S, Frahm J. Single-shot multi-slice T1 mapping at high spatial resolution—inversion-recovery FLASH with radial undersampling and iterative reconstruction. *Open Med Imaging J* 2015; **9**: 1–8. doi: <https://doi.org/10.2174/1874347101509010001>
- Hofer S, Wang X, Roeloffs V, Frahm J. Single-shot T1 mapping of the corpus callosum: a rapid characterization of fiber bundle anatomy. *Front Neuroanat* 2015; **9**: 57. doi: <https://doi.org/10.3389/fnana.2015.00057>

12. Zhang S, Uecker M, Voit D, Merboldt KD, Frahm J. Real-time cardiovascular magnetic resonance at high temporal resolution: radial FLASH with nonlinear inverse reconstruction. *J Cardiovasc Magn Reson* 2010; **12**: 39. doi: <https://doi.org/10.1186/1532-429X-12-39>
13. Voit D, Zhang S, Unterberg-Buchwald C, Sohns JM, Lotz J, Frahm J. Real-time cardiovascular magnetic resonance at 1.5 T using balanced SSFP and 40 ms resolution. *J Cardiovasc Magn Reson* 2013; **15**: 79. doi: <https://doi.org/10.1186/1532-429X-15-79>
14. Untenberger M, Tan Z, Voit D, Joseph AA, Roeloffs V, Merboldt KD, et al. Advances in real-time phase-contrast flow MRI using asymmetric radial gradient echoes. *Magn Reson Med* 2016; **75**: 1901–8. doi: <https://doi.org/10.1002/mrm.25696>
15. Zhang S, Joseph AA, Voit D, Schaetz S, Merboldt KD, Unterberg-Buchwald C, et al. Real-time magnetic resonance imaging of cardiac function and flow—recent progress. *Quant Imaging Med Surg* 2014; **4**: 313–29. doi: <https://doi.org/10.3978/j.issn.2223-4292.2014.06.03>
16. Roeloffs V, Voit D, Frahm J. Spoiling without additional gradients: radial FLASH MRI with randomized radiofrequency phases. *Magn Reson Med* 2016; **75**: 2094–9. doi: <https://doi.org/10.1002/mrm.25809>
17. Frahm J, Schätz S, Untenberger M, Zhang S, Voit D, Merboldt KD, et al. On the temporal fidelity of nonlinear inverse reconstructions for real-time MRI—the motion challenge. *Open Med Imaging J* 2014; **8**: 1–7. doi: <https://doi.org/10.2174/1874347101408010001>
18. Klosowski J, Frahm J. Image denoising for real-time MRI. *Magn Reson Med* 2016; doi: <https://doi.org/10.1002/mrm.26205>
19. Nocedal J, Wright SJ. Numerical Optimization. In: Mikosch TV, Sidney S, Resnick I, Robinson SM, eds. *Springer Series in Operations Research*. New York, NY: Springer Science+Business Media; 2006. pp. 66–98.
20. King D. Dlib-ml: A Machine Learning Toolkit. *J Mach Learn Res* 2009; **10**: 1755–1758.
21. Deichmann R. Fast high-resolution T1 mapping of the human brain. *Magn Reson Med* 2005; **54**: 20–7. doi: <https://doi.org/10.1002/mrm.20552>
22. Sumpf T, Unterberger M. arrayShow: a guide to an open source matlab tool for complex MRI data analysis. In: *ISMRM*; 2013. p. 2719.
23. Kawel N, Nacif M, Zavodni A, Jones J, Liu S, Sibley CT, et al. T1 mapping of the myocardium: intra-individual assessment of the effect of field strength, cardiac cycle and variation by myocardial region. *J Cardiovasc Magn Reson* 2012; **14**: 27. doi: <https://doi.org/10.1186/1532-429X-14-27>
24. von Knobelsdorff-Brenkenhoff F, Prothmann M, Dieringer MA, Wassmuth R, Greiser A, Schwenke C, et al. Myocardial T1 and T2 mapping at 3 T: reference values, influencing factors and implications. *J Cardiovasc Magn Reson* 2013; **15**: 53. doi: <https://doi.org/10.1186/1532-429X-15-53>
25. Lee JJ, Liu S, Nacif MS, Ugander M, Han J, Kawel N, et al. Myocardial T1 and extracellular volume fraction mapping at 3 Tesla. *J Cardiovasc Magn Reson* 2011; **13**: 75. doi: <https://doi.org/10.1186/1532-429X-13-75>
26. Shao J, Rapacchi S, Nguyen KL, Hu P. Myocardial T1 mapping at 3.0 Tesla using an inversion recovery spoiled gradient echo readout and Bloch equation simulation with slice profile correction (BLESSPC) T1 estimation algorithm. *J Magn Reson Imaging* 2016; **43**: 414–25. doi: <https://doi.org/10.1002/jmri.24999>
27. Gensler D, Mörchel P, Fidler F, Ritter O, Quick HH, Ladd ME, et al. Myocardial T1: quantification by using an ECG-triggered radial single-shot inversion-recovery MR imaging sequence. *Radiology* 2015; **274**: 879–87. doi: <https://doi.org/10.1148/radiol.14131295>
28. Mehta BB, Chen X, Bilchick KC, Salerno M, Epstein FH. Accelerated and navigator-gated look-locker imaging for cardiac T1 estimation (ANGIE): development and application to T1 mapping of the right ventricle. *Magn Reson Med* 2015; **73**: 150–60. doi: <https://doi.org/10.1002/mrm.25100>
29. Sumpf TJ, Petrovic A, Uecker M, Knoll F, Frahm J. Fast T2 mapping with improved accuracy using undersampled spin-echo MRI and model-based reconstructions with a generating function. *IEEE Trans Med Imaging* 2014; **33**: 2213–22. doi: <https://doi.org/10.1109/TMI.2014.2333370>